



Deglacial and Holocene archaeal lipid-inferred paleohydrology and paleotemperature history of Lake Qinghai, northeastern Qinghai–Tibetan Plateau



Huanye Wang^{a,b,c}, Hailiang Dong^{d,e}, Chuanlun L. Zhang^{f,g}, Hongchen Jiang^h, Zhonghui Liuⁱ, Meixun Zhao^j, Weiguo Liu^{a,k,*}

^a State Key Laboratory of Loess and Quaternary Geology, IEE, CAS, Xi'an 710075, China

^b Key Laboratory of Salt Lake Resources and Chemistry, Qinghai Institute of Salt Lake, Chinese Academy of Sciences, Xining, Qinghai 810008, China

^c University of Chinese Academy of Sciences, Beijing 100049, China

^d State Key Laboratory of Biogeology and Environmental Geology, China University of Geosciences, Beijing, 100083, China

^e Department of Geology and Environmental Earth Science, Miami University, Oxford, OH 45056, USA

^f State Key Laboratory of Marine Geology, Tongji University, Shanghai 200092, China

^g Department of Marine Sciences, The University of Georgia, Athens, GA 30602, USA

^h State Key Laboratory of Biogeology and Environmental Geology, China University of Geosciences, Wuhan 430074, China

ⁱ Department of Earth Sciences, The University of Hong Kong, Hong Kong, China

^j Key Laboratory of Marine Chemistry Theory and Technology (Ocean University of China), Ministry of Education/Qingdao Collaborative Innovation Center of Marine Science and Technology, Qingdao 266100, China

^k School of Human Settlement and Civil Engineering, Xi'an Jiaotong University, Xi'an 710049, China

ARTICLE INFO

Article history:

Received 9 August 2014

Available online 18 November 2014

Keywords:

Archaeal lipids

Thaumarchaeol

ACE

TEX₈₆

Lake level

Salinity

Paleotemperature

Paleoclimate patterns

Lake Qinghai

Qinghai–Tibetan Plateau

ABSTRACT

We investigate the distribution of archaeal lipids in a 5.8-m-long sedimentary core recovered from Lake Qinghai to extract regional hydroclimate and temperature signals since the last deglaciation for this important region. The paleohydrology was reconstructed from the relative abundance of thaumarchaeol (%*thaum*) and the archaeal and caldarchaeol ecometric (ACE) index. The %*thaum*-inferred lake-level record was extended to deglaciation, showing three periods (11.9–13.0, 14.1–14.7 and 15.1–17.2 cal ka BP) with relatively higher lake levels than those during the early Holocene. The ACE record demonstrates three periods (10.6–11.2, 13.2–13.4 and 17.4–17.6 cal ka BP) of elevated salinity when the lake was shallow. Filtered TEX₈₆ record based on archaeal lipid distributions corresponded to relatively higher lake levels, implying that a certain lake size is required for using the TEX₈₆ paleothermometer. At 1–4 cal ka BP, the reconstructed temperature fluctuated significantly and correlated negatively with inferred lake level, indicating that lake temperature and hydrological change might be coupled during this period. We attribute this co-variance to the importance of summer temperature in controlling evaporation for this arid/semi-arid region. Moreover, our results indicate that archaeal lipids have potential in reconstructing paleoclimate patterns from lacustrine sedimentary cores, but the data should be interpreted with care.

© 2014 University of Washington. Published by Elsevier Inc. All rights reserved.

Introduction

Understanding past terrestrial climate variation is important for assessing modern and future climate variability. Lipid biomarkers preserved in dated lacustrine deposits are generally valuable indicators of past climate change, especially for the Quaternary (Castañeda and Schouten, 2011; Sinninghe Damsté et al., 2012a). Molecular proxies have, however, been less commonly applied to lacustrine sedimentary records than their wide use in marine systems, due to the complex

physical and chemical properties of lakes and the limited fundamental research aimed at developing molecular proxies for use in lacustrine settings (Castañeda and Schouten, 2011).

Isoprenoid glycerol ethers (Fig. 1), the membrane lipids of Archaea, are one group of the most abundant and ubiquitous lipids on earth. They have been increasingly used in paleoenvironmental reconstructions since they are easy-to-analyze and their relative abundance is sensitive to environmental variables (Castañeda and Schouten, 2011; Schouten et al., 2013). A few years ago, Schouten et al. (2002) found that the TEX₈₆ index, representing the relative distribution of cyclopentane rings in isoprenoid glycerol dialkyl glycerol tetraethers (iGDGTs) biosynthesized mainly by aquatic Thaumarchaeota (previously called mesophilic Crenarchaeota, Brochier-Armanet et al., 2008), had a

* Corresponding author at: State Key Laboratory of Loess and Quaternary Geology, IEE, CAS, Xi'an 710075, China.

E-mail address: liuwg@loess.llqg.ac.cn (W. Liu).

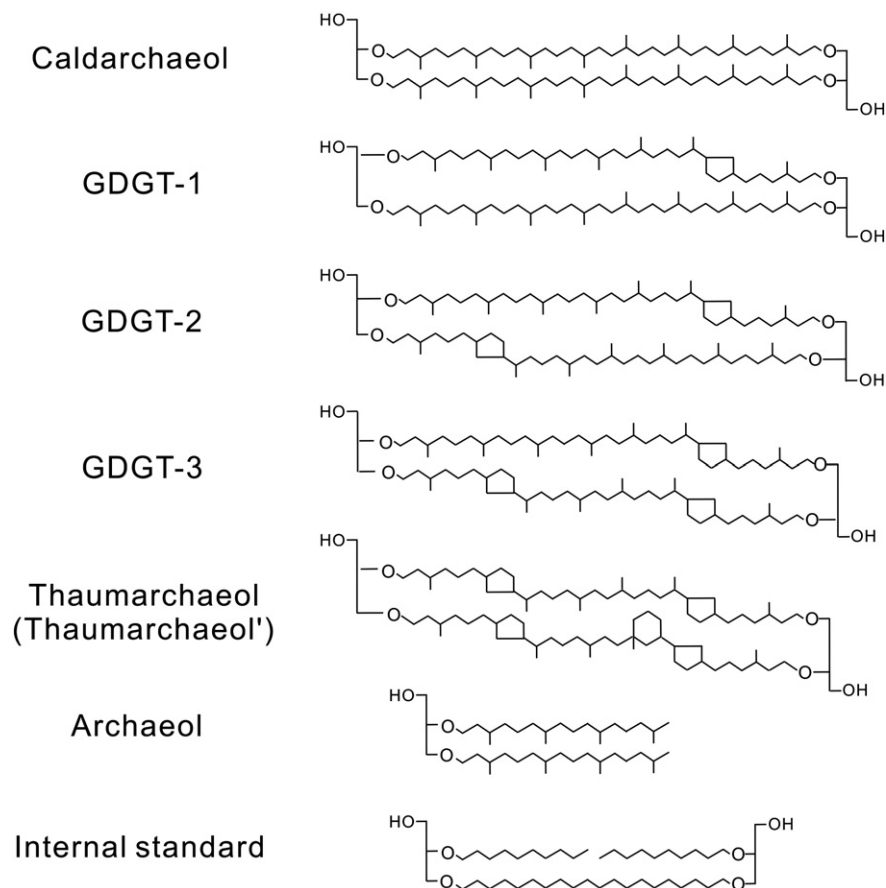


Figure 1. Structures of archaeal lipids and internal standard discussed in the text.

linear relationship with sea-surface temperature in core-top marine sediments. However, despite the successful application of TEX₈₆ to marine sediments (e.g., Schouten et al., 2003; Zachos et al., 2006; Liu et al., 2009; Pearson and Ingalls, 2013), subsequent lacustrine studies indicated that the index might only serve as a paleothermometer in limited lacustrine systems (Powers et al., 2004, 2010; Blaga et al., 2009), predominately certain large African lakes (Powers et al., 2005; Tierney et al., 2008, 2010a; Woltering et al., 2011; Berke et al., 2012a, b; Ménot and Bard, 2012). For other lakes, it might be applicable only when the influence of GDGTs originating from soil archaea and/or other groups of archaea living in the lake (e.g., methanotrophic or methanogenic archaea) was excluded (Blaga et al., 2009; Sinninghe Damsté et al., 2012a).

The distributions of archaeal lipids also have potentials in paleohydrological studies. Thaumarchaeol (also named crenarchaeol), a unique GDGT specific for Thaumarchaeota (Sinninghe Damsté et al., 2002; Brochier-Armanet et al., 2008; Pitcher et al., 2010; Spang et al., 2010), has recently been proposed as a potential tool for evaluating lake-level changes, particularly for lakes with medium size and depth (Wang et al., 2014). This is based on the empirical relationship between thaumarchaeol abundance (%thaum) and in situ lake water depth observed for core-top sediments collected from East African lake groups (Tierney et al., 2010b) and Lake Qinghai (Wang et al., 2014), and is supported by the consistency of the %thaum record with the carbon isotope of bulk organic carbon ($\delta^{13}\text{C}_{\text{org}}$, a water depth indicator in Lake Qinghai) record in sediment cores. Since the four TEX₈₆-related GDGTs (if TEX₈₆ works) and thaumarchaeol are both produced by Thaumarchaeota, it seems promising to retrieve paired information on changes in temperature and hydrological conditions in the same sediment core, unaffected by chronology uncertainty.

In addition, Turich and Freeman (2011) proposed the ACE index as a tracer of water salinity, because the relative abundance of archaeol to caldarchaeol (also called GDGT-0) reflected changes in archaeal community structure in response to variations in salinity in modern settings. This was corroborated by a similar study (Wang et al., 2013) of modern inland lakes on the Qinghai–Tibetan Plateau (QTP). Because Archaea can survive and thrive over a broad salinity range, the ACE index might be promising for paleosalinity reconstruction, especially for hypersaline waters with few haptophyte algae and other planktons (Turich and Freeman, 2011; Wang et al., 2013). Currently, however, the ACE index has not been applied in paleoenvironmental studies of inland lakes.

Lake Qinghai (Fig. 2), located at the transition from the arid to the semi-arid climate zones, is the largest interior plateau lake in Central Asia (Fu et al., 2013). Due to the sensitivity of its regional climate to monsoon variation and global change (Shi et al., 1958; Zhang et al., 1989; Ji et al., 2005; Shen et al., 2005; An et al., 2012; Liu et al., 2013a), paleoclimate reconstructions from Lake Qinghai are of wide interest for understanding how complex forcing mechanisms could affect the regional climate (Liu et al., 2006; An et al., 2012). This is also reflected by the recent deep drilling of the lake as part of the International Continental Scientific Drilling Program (Henderson and Holmes, 2009). Numerous paleoclimate records from Lake Qinghai have been published during the past three decades (e.g., Zhang et al., 1989; Lister et al., 1991; Ji et al., 2005; Shen et al., 2005; Yu, 2005; Colman et al., 2007; Henderson et al., 2010; Liu et al., 2011a; Lu et al., 2011; An et al., 2012; Li and Liu, 2014). However, the paleoclimate history and climate pattern for the lake is still controversial on both short and long timescales, mainly due to uncertainties in age models and over proxy interpretations (Henderson and Holmes, 2009). Moreover, our knowledge of the quantitative paleotemperature history of Lake

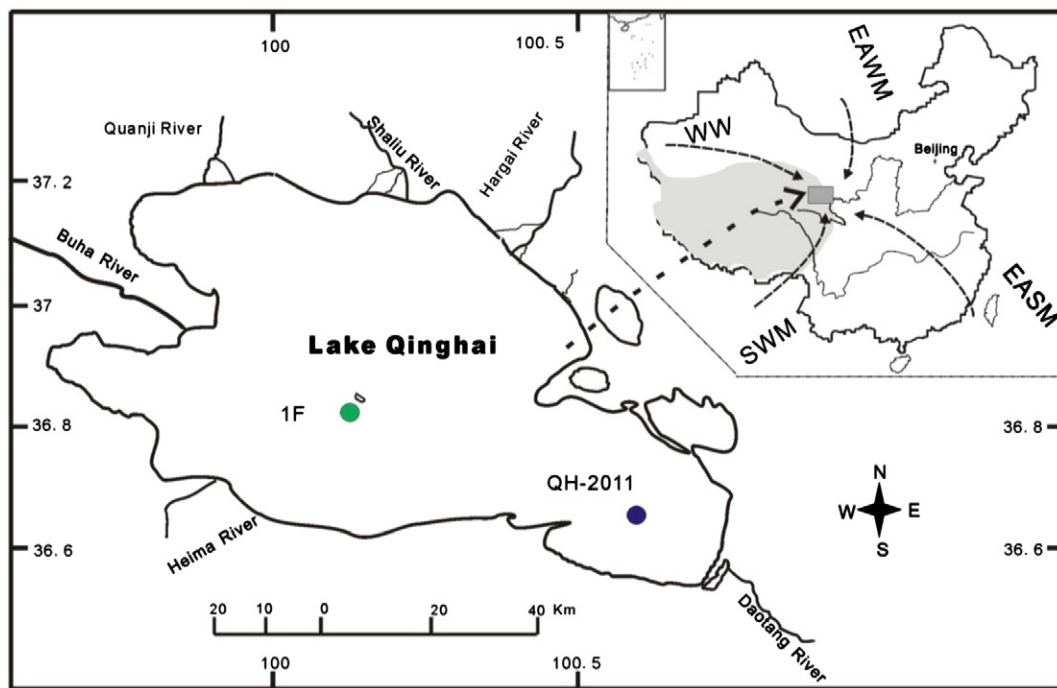


Figure 2. The map of coring site (QH-2011) with atmospheric circulation patterns of the Lake Qinghai region. Core 1F (An et al., 2012; Liu et al., 2013a) in the southwestern sub-basin is also indicated. EASM, EAWM, WW and SWM are abbreviations for East Asian Summer Monsoon, East Asian Winter Monsoon, Westerly Wind, and Southwest Monsoon, respectively (after Wang et al., 2014).

Qinghai is mainly based on the alkenone unsaturation index (U_{37}^{alk}) and is limited to the past 3.5 ka (Liu et al., 2006).

Given the potentials of archaeological lipids in paleoclimate reconstructions on the QTP (Wang et al., 2012, 2013, 2014; Günther et al., 2014), we investigate the distribution of iGDGTs in a 5.8-m-long core from Lake Qinghai, covering the past ca. 18 ka. The aim is to provide further insight into the paleohydrological history and extract reliable paleotemperature signals for this geologically important region since the late glacial period. The lake-level and salinity changes were reconstructed from the $\delta^{18}O$ and the ACE index, respectively. The TEX_{86} temperature signals were extracted by applying an approach similar to that of Sinninghe Damsté et al. (2012a). Finally, the regional climate pattern (i.e., temperature–moisture association) of the late Holocene is discussed by comparing the extracted temperature signals with the $\delta^{18}O$ -inferred lake-level variation.

Materials and methods

Study site and sampling

Lake Qinghai (36°32' to 37°15'N, 99°36' to 100°47'E; Fig. 2) is a brackish to saline (14–16 g/l, dominated by Na and Cl), alkaline (pH 8.8–9.3; Xu et al., 2010) and closed-basin lake on the northeastern QTP, China. The lake is surrounded by mountains such as Datongshan, Riyueshan and Nanshan (Liu et al., 2011b). It has an altitude of 3193 m, surface area of 4400 km² and average water depth of 21 m. The maximum water depth (ca. 27 m) occurs in the south basin (Henderson and Holmes, 2009). A cold and semi-arid continental climate prevails in the entire lake basin. The wind blows onshore in the day and offshore at night, with an average speed of 4–6 m/s (Colman et al., 2007). Based on a 10-yr (1994–2004) instrumental record from a meteorological station 50 km to the north of the lake, mean annual air temperature is 0.24°C (Liu et al., 2008). In summer, weak thermal stratification occurs (thermocline at 10–15 m), with the epilimnion at 12–15°C and the hypolimnion at 6°C (Lister et al., 1991; Williams, 1991). The mean July lake surface temperature (JLST) is ca. 14.3°C (Fan et al., 1994). The freeze-up period is ca. 3 to 4 months

(December–March) each year, with a maximum ice thickness of 0.8 m (Colman et al., 2007). The mean annual precipitation is 250–400 mm for the region (Shen et al., 2005; Wang et al., 2012), most of which falls in summer, showing a clear seasonality of monsoonal precipitation (An et al., 2012). However, evaporation (800–1200 mm) is 3–4 times greater than precipitation. Rivers draining to the lake lie mainly on the north and northwest, with Buha River the largest (LZBCAS, 1994). The residence time of the lake water is ca. 33.4 yr (Lister et al., 1991).

A 5.8-m-long core (QH-2011) was retrieved from the southeastern sub-basin of the lake in August 2011 at a water depth of ca. 24 m (Wang et al., 2014). An age–depth model was established by Wang et al. (2014; Fig. 3), based on six converted calendar years (using the IntCal13 calibration curve, Reimer et al., 2013) framed by reservoir effect-corrected AMS ¹⁴C ages for bulk organic carbon samples, in addition to 6 calendar ages from core QH-2005 retrieved from a similar site in the southeastern sub-basin (Wang et al., 2011). Approximately

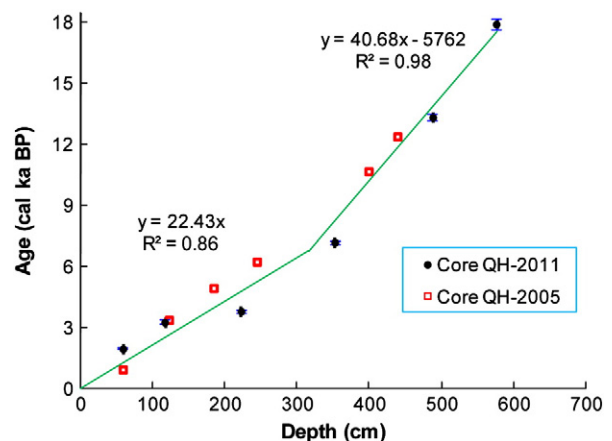


Figure 3. The chronology for core QH-2011, based on converted age of this core (Wang et al., 2014) and core QH-2005 (Wang et al., 2011). Two regression lines were built for the first 8 ages and last 4 ages, respectively. They cross at 312–313 cm (modified from Wang et al., 2014).

190 samples were used for GDGT analysis, resulting in an average sampling resolution of ca. 100 yr.

Lipid analysis

Briefly, 1–5 g freeze-dried samples were extracted ultrasonically using MeOH, MeOH/dichloromethane (DCM) (1:1, v/v), DCM, MeOH/DCM (1:1, v/v) and MeOH, respectively (Wang et al., 2012), following the method modified from Schouten et al. (2007). A known amount of C₄₆ GDGT internal standard (IS, Huguet et al., 2006) was added to the combined extract, which was then dried under N₂, re-dissolved in hexane/isopropanol (99:1 v/v) and filtered through a 0.45 μm PTFE syringe filter prior to injection for GDGT measurement.

GDGTs were analyzed using high performance liquid chromatography/atmospheric pressure chemical ionization–mass spectrometry (HPLC–APCI–MS) with an Agilent 1200 HPLC instrument connected to a QQQ 6460 mass spectrometer as described by Zhang et al. (2012), slightly modified from Hopmans et al. (2000) and Schouten et al. (2007). Scanning was performed in selected ion monitoring (SIM) mode to target specific *m/z* values for archaeol and each GDGT. Structures and [M + H]⁺ *m/z* values for these lipids are shown in Figure 1.

The %thaum values were calculated as follows:

$$\% \text{thaum} = \text{thaum} / (\text{GDGT-0} + \text{GDGT-1} + \text{GDGT-2} + \text{GDGT-3} + \text{thaum} + \text{thaum}'). \quad (1)$$

The ACE index was calculated according to Wang et al. (2013):

$$\text{ACE} = (\text{archaeol}/10) / (\text{archaeol}/10 + \text{GDGT-0}) \times 100. \quad (2)$$

The methane index (MI) was calculated following Zhang et al. (2011):

$$\text{MI} = \frac{\text{GDGT-1} + \text{GDGT-2} + \text{GDGT-3}}{\text{GDGT-1} + \text{GDGT-2} + \text{GDGT-3} + \text{Thaum} + \text{Thaum}'}. \quad (3)$$

TEX₈₆ was calculated according to Schouten et al. (2002):

$$\text{TEX}_{86} = \frac{\text{GDGT-2} + \text{GDGT-3} + \text{Thaum}'}{\text{GDGT-1} + \text{GDGT-2} + \text{GDGT-3} + \text{Thaum}'}. \quad (4)$$

TEX₈₆-inferred lake surface temperature (LST) was calculated using the global lake calibration of Powers et al. (2010):

$$\text{LST} = 55.231 \times \text{TEX}_{86} - 13.955. \quad (5)$$

Results

A wide variety of iGDGT composition was found. The %thaum index ranged from 0.6% to 66.6%. Besides the reported late Holocene high %thaum stage (Wang et al., 2014), relatively higher %thaum values also occurred at 11.9–12.9, 14.1–14.8 and 15.3–17.3 cal ka BP during the deglacial period (Fig. 4a).

The ACE record exhibited a negative relationship with the %thaum record. ACE values ranged from 0.1 to 65.8, with three pulses of high values (>5) at 10.5–11.2, 13.2–13.3 and 17.5–17.6 cal ka BP, respectively. Moreover, two periods with the lowest ACE values (<0.5) were found at 0–3.5 and 15.2–17.0 cal ka BP, respectively (Fig. 4b).

The abundance of GDGT-0 relative to thaumarchaeol (GDGT-0/thaum) ranged from 0.36 to 148. The ratio was <2 from 0 to 5 cal ka BP, mostly >2 with significant fluctuation within 5–12 cal ka BP, 0.70–1.33 at 12–13 cal ka BP, 1.78–6.92 at 13–14 cal ka BP and mainly <2 from 14 to 18 cal ka BP (Fig. 4c; note the log scale). In particular, two periods with lowest GDGT-0/thaum ratio were found at 4.7–5.0 and 15.6–16.8 cal ka BP (Fig. 4c).

The MI index varied between 0.07 and 0.95 (Fig. 4d). About half of the samples analyzed between 6.9 and 11.5 cal ka BP (18 of 41) are not reported for MI values, as GDGTs 1–3 used for the calculation were interfered by unknown peaks (early and late eluting lipids, most likely their isomers; cf. Pitcher et al., 2010, 2011) in the HPLC chromatograms. Regardless of these samples, the highest MI values occurred between 9 and 11 cal ka BP, while MI values were persistently lowest in the recent 3.7 ka.

The %thaum isomer, defined as the relative amount of the thaumarchaeol isomer to the sum of thaumarchaeol and its isomer, showed rather similar variation to that for the GDGT-0/thaum ratio, with lower %thaum isomer (<1%) at 4.7–5, 8.4, 14.1–14.4 and 15.7–17.0 cal ka BP (Fig. 4e; note the log scale); 17 samples, mostly at 6.9–11.5 cal ka BP, are not reported for their %thaum isomer values, as a result of low thaum isomer abundance.

The TEX₈₆ values also exhibited significant variability, ranging from 0.34 to 0.76 (Fig. 4f). They decreased from 0.54 to 0.34 at 17.5–16.4 cal ka BP, increased to 0.71 from 16.3 to 10.8 cal ka BP, varied between 0.37 and 0.76 from 10.8 to 5.0 cal ka BP and fluctuated at around 0.5 from 0 to 5 cal ka BP. Again, about half of the samples analyzed between 6.9 and 11.5 cal ka BP (18 of 41) are not reported for TEX₈₆ values, owing mainly to the inadequate separation of co-eluting isomers for TEX₈₆-related GDGTs 1–3, as well as the low abundance of thaum'.

Discussion

Paleohydrology of Lake Qinghai

Lake-level variation based on %thaum

Preliminary application of the %thaum proxy to the upper 4.35 m of the core revealed an expanding lake from the early to the late Holocene, in good agreement with the lake-level history inferred from δ¹³C_{org} values (Figs. 5a, b; Liu et al., 2013a; Wang et al., 2014). There is, however, no report of a continuous lake-level history for the lake during deglaciation. In the following, we further explored the pre-Holocene relative lake-level history according to the positive %thaum–depth relationship presented by Wang et al. (2014).

It appears that the lake was deeper during much of the time in the deglaciation (ca. 11.7–17.7 cal ka BP) than at the early Holocene (Fig. 5a). The lake was shallow at the start of this record but expanded rapidly within ~400 yr. After a highstand between 15.1 and 17.3 cal ka BP, it was decreasing to the early-Holocene lowstand interrupted by two periods of relatively higher lake level at 14.1–14.8 cal ka BP and 11.9–13.0 cal ka BP (Fig. 5a). It might be argued that archaeal GDGTs in the lake could come from eolian dust during the pre-Holocene period, provided that the regional climate were cold and dry as a result of the weak Asian summer monsoon and strong westerly (Shen et al., 2005; An et al., 2012). If this was the case, %thaum might fail to indicate lake level variations due to the substantially external thaumarchaeol input from soils. However, some fine-grained layers with a significant decreases in the content of >25 μm fraction (an indicator of the eolian contribution to the sediments of Lake Qinghai; An et al., 2012) have actually been observed for the pre-Holocene sediments of cores 1A and 1F, suggesting that some humid intervals with low eolian input during deglaciation might exist for this region (An et al., 2012). More importantly, we also note that the distributions of archaeal GDGTs (TEX₈₆, Fig. 6a; %thaum isomer, Fig. 6b) at the three pre-Holocene periods with relatively higher inferred lake levels (11.9–12.9, 14.1–14.8 and 15.3–17.3 cal ka BP) were quite different from that in modern soils surrounding the lake (Wang et al., 2012) and on nearby Mt. Xiangpi (Liu et al., 2013b). This indicates that archaeal lipids were mainly produced in situ in the lake during these intervals. Therefore, we think that a medium to large Lake Qinghai during certain deglaciation periods was possible.

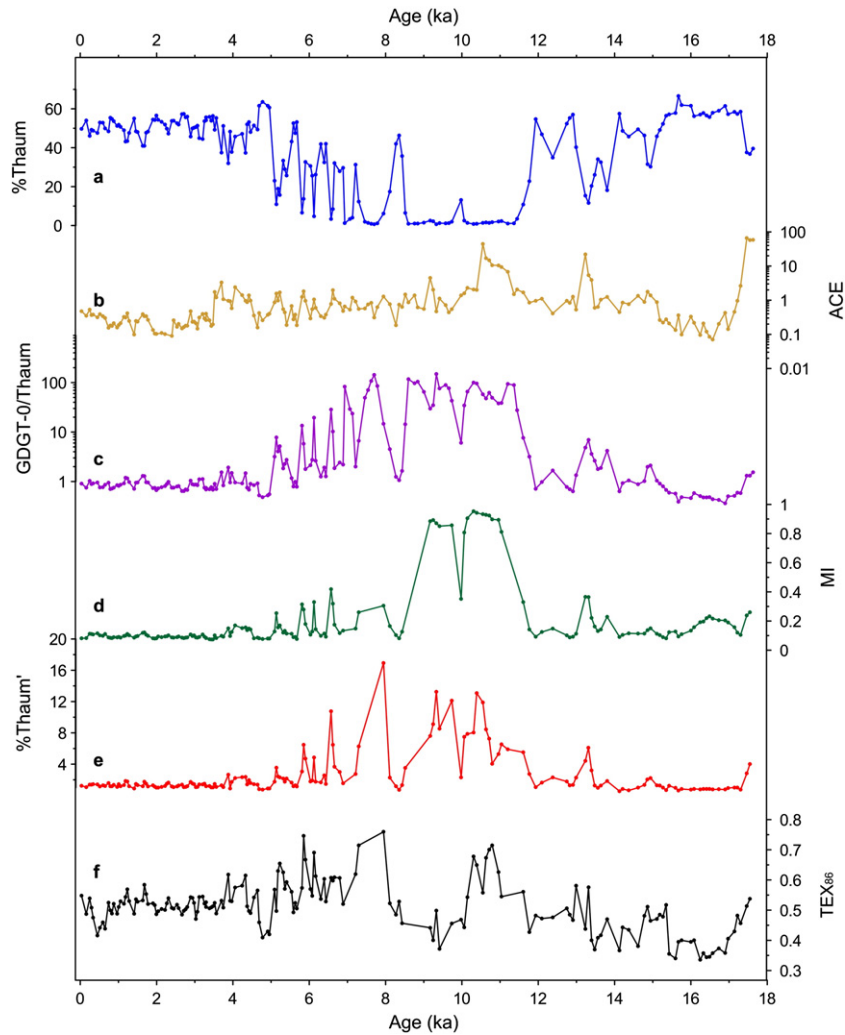


Figure 4. Multi-proxy records from core QH-2011 at Lake Qinghai: (a) %thaum (0–12 cal ka BP; Wang et al., 2014); (b) ACE; (c) GDGT-0/thaum ratio; (d) %thaum isomer; (e) MI and (f) TEX₈₆.

The highstand for the lake at 15.3–17.3 cal ka BP would be caused either by low water loss or by high water input. For the closed basin Lake Qinghai, the main cause to water loss is evaporation. Therefore, the regional cold climate at that time (as inferred from the low TEX₈₆ values, section 4.2) would have resulted in a low evaporation rate and thus high moisture condition. Alternatively, high precipitation or runoff caused by snow/glacier melting would be potentially responsible for the pre-Holocene highstand. High precipitation at this period, however, seems less likely when viewed in the context of the continuously weak Asian summer monsoon prior to the Holocene (An et al., 2012). On the other hand, continental temperature reconstructions from the western QTP (Thompson et al., 1997) and the nearby Chinese Loess Plateau (Peterse et al., 2011; Gao et al., 2012; Jia et al., 2013; Yang et al., 2014) both indicate that the rapid deglacial warming might have started at least since ~19 ka and lasted until ~14 ka. Considering that the lake was surrounded by several high mountains that might have been covered by massive glaciers and snow during the last glacial maximum, the input of meltwater resulting from increasing land temperature may account for the highstand at 15.3–17.3 cal ka BP. More evidences from other aspects (e.g., the local land temperature record or evidence for snow melting) would further constrain the pre-Holocene lake status of Lake Qinghai and its causes.

Salinity variation based on ACE

Changes in lake-water salinity during short timescales generally correspond to lake-level variations at a specific closed-lake system (e.g., De Deckker and Forester, 1988 and Mischke et al., 2008). As shown previously, the lake level of Lake Qinghai might have fluctuated severely since the deglaciation. Such abrupt fluctuations in lake level could, in consequence, induce profound changes in water chemistry for this closed-basin lake. Therefore, the newly proposed ACE index (Turich and Freeman, 2011) was also utilized to reconstruct relative changes in salinity in the same period, in an effort to test its applicability for ancient lake deposits and to obtain a more comprehensive hydrological evolution history at Lake Qinghai.

The ACE record revealed pronounced variability in paleosalinity. The remarkable high ACE values at 10.5–11.2, 13.2–13.3 and 17.5–17.6 cal ka BP in Figure 5c indicated the three saltiest episodes for the past 18 ka, which were in accord with the inferred relatively lower lake levels at 10.1–11.4, 13.2–13.8 and 17.5–17.6 cal ka BP, respectively. On the other hand, two periods with lowest ACE values (0–3.5 and 15.2–17.0 cal ka BP) represented relatively fresher water stages, coinciding with the inferred relatively higher lake levels at both intervals (Figs. 5a, c). Such a correspondence between the two hydrological proxies supports the application of ACE as a salinity indicator when

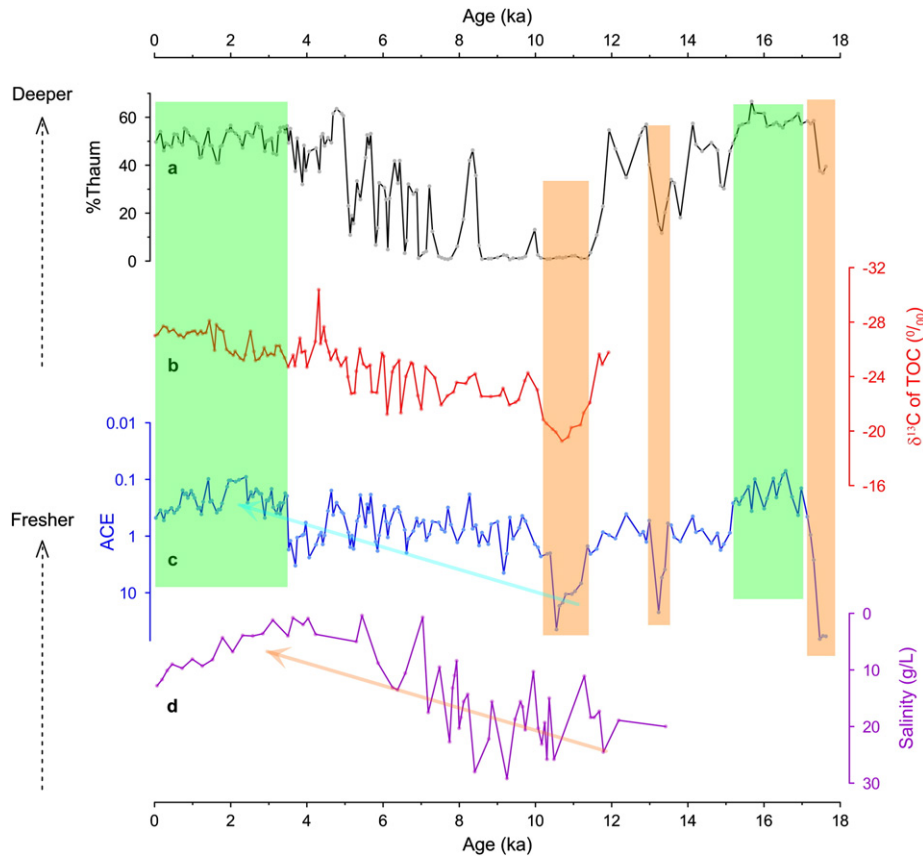


Figure 5. Paleohydrology of Lake Qinghai recorded in core QH-2011 and QH-16A. (a) Relative lake-level history inferred from %thaum (0–12 cal ka BP; Wang et al., 2014). (b) A 12-ka relative lake-level history inferred from $\delta^{13}C_{org}$ (Wang et al., 2014). (c) Relative salinity history inferred from the ACE index. (d) Reconstructed salinity record of core QH-16A based on Sr/Ca of fossil ostracods (Zhang et al., 1994). Periods with lower salinity and higher lake level are highlighted with green shadings, while orange shadings indicate 3 periods with relatively higher salinity.

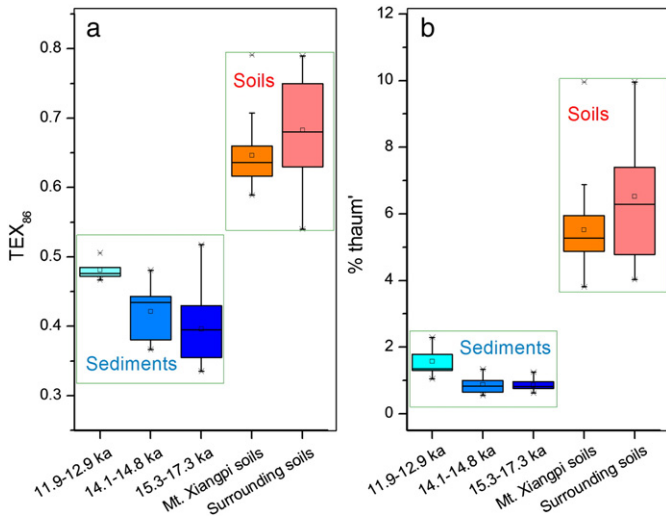


Figure 6. Comparison of TEX_{86} and %thaum isomer values between the three pre-Holocene intervals (11.9–12.9, 14.1–14.8 and 15.3–17.3 cal ka BP) with relatively higher lake levels and the nearby modern surface soils of Lake Qinghai (Wang et al., 2012; Liu et al., 2013b). The box-and-whisker plots show the 25th (bottom of the box) and 75th (top of the box) percentile (the lower and upper quartiles), while the line in the middle of the boxes represents the median (50th percentile). The whiskers (error bars) above and below the box indicate the 90th and 10th percentiles, respectively. The minimum and maximum values are indicated as small grayish tick marks.

the salinity varied within a large range (Turich and Freeman, 2011), and confirms the %thaum-inferred relative lake-level history.

Our ACE record is also in reasonable agreement with the trend in Holocene salinity history reconstructed from the trace metals (Sr/Ca) (Zhang et al., 1994; Fig. 5d) and species composition (Li and Liu, 2014) of fossil ostracods, considering differences in age model and sampling resolution. All records show that the lake water had a much higher salinity in the early Holocene and gradually became fresher towards the mid- and late Holocene. Moreover, the fluctuations in ACE values generally resembled lake-level variations inferred from the %thaum index and $\delta^{13}C_{org}$ at periods with relatively lower ACE values in core QH-2011 (Figs. 5a–c). However, we observed some inconsistencies between lake-level and salinity reconstructions during 7–10 cal ka BP. This is possibly because that the ACE index is not so sensitive to salinity in small, fresh and fresh-to-brackish lakes. Indeed, in modern marine and lacustrine environments, it seems that the correlation between water salinity and the ACE index is less obvious at lower salinity range (Turich and Freeman, 2011; Wang et al., 2013; Günther et al., 2014), compared with the significant correlation over the whole salinity range. Therefore, small variation of ACE at low values in a single sediment core should be interpreted with care as salinity changes.

Extracting the paleotemperature signals for Lake Qinghai

The proper application of TEX_{86} as a lacustrine paleotemperature proxy is critically based on the premise that the four TEX_{86} -related

GDGTs are derived predominantly from Thaumarchaeota living in the water column (Sinninghe Damsté et al., 2012a). However, iGDGTs originating from other groups of archaea within the lake (e.g., methanotrophic or methanogenic archaea), and/or the input of soil-derived iGDGTs, could complicate the application of TEX_{86} for many lakes (Blaga et al., 2009; Sinninghe Damsté et al., 2009, 2012a; Powers et al., 2010; Pearson et al., 2011; Schouten et al., 2013). Therefore, careful screening was required before applying TEX_{86} to core QH 2011, as the hydrological status of Lake Qinghai (and thus the sources of iGDGTs) may have changed greatly in the past 18 ka.

First, the relative distribution of iGDGTs might be biased by methanotrophic Euryarchaeota since they appear to produce not only GDGT-0 but also substantial amounts of GDGTs 1–4 (Pancost et al., 2001; Wakeham et al., 2003; Zhang et al., 2003, 2011; Blumenberg et al., 2004; Schouten et al., 2013). The imprint from methanotrophic Euryarchaeota can be assessed by the so-called MI (Zhang et al., 2011), which varies within the range 0 to 0.3 in normal marine conditions, with the majority of values between 0.03 and 0.24 (Kim et al., 2010; Zhang et al., 2011). Extrapolated from the MI–temperature relationship for normal marine surface sediments derived in Zhang et al. (2011), a hypothetical 40°C high temperature could only give a MI value of 0.26. Therefore, high MI values may point to a contribution of GDGTs from methanotrophic Euryarchaeota in lake sediments.

Methanogenic Euryarchaeota, which could potentially generate some of the same iGDGTs as Thaumarchaeota (Schouten et al., 2013 and references therein) but lack the appropriate relationship with temperature, are likely to affect TEX_{86} as well in lacustrine systems. GDGT-0 is a common membrane lipid of Archaea, whereas thaumarchaeol is considered specific for Thaumarchaeota (Brochier-Armanet et al., 2008; Pitcher et al., 2010; Spang et al., 2010) which produce relatively lower GDGT-0 (e.g., Pitcher et al., 2011). Therefore, the GDGT-0/thaum ratio, generally between 0.2 and 2 for Thaumarchaeota (Schouten et al., 2002), can be used as an empirical criterion for evaluating the influence of methanogenic Euryarchaeota or methanotrophic Euryarchaeota, where a ratio >2 indicates a substantial methanogenic or methanotrophic archaea origin (Blaga et al., 2009; Pearson et al., 2011).

Furthermore, the application of TEX_{86} is also problematic for lakes with a significant input of GDGTs from catchment soils (e.g., Blaga et al., 2009; Powers et al., 2010; Schouten et al., 2012), because iGDGTs used to calculate TEX_{86} are also present in various amounts in soils (Weijers et al., 2006; Huguet et al., 2010; Wang et al., 2012; Xie et al., 2012; Yang et al., 2012; Liu et al., 2013b). Interestingly, %thaum isomer is obviously different between soil GDGTs and those produced by aquatic Group I.1a Thaumarchaeota (Sinninghe Damsté et al., 2012a, b). The %thaum isomer for enrichment cultures of Group I.1a aquatic Thaumarchaeota is 3% on average (Pitcher et al., 2011). In contrast, Group I.1b Thaumarchaeota, which is generally abundant in soil, produces GDGTs with %thaum isomer values typically >20% (Pitcher et al., 2010; Sinninghe Damsté et al., 2012b). Consequently, %thaum isomer values for soils are generally higher than those produced by Group I.1a aquatic Thaumarchaeota. For example, the average %thaum isomer value for global soils and soils around Lake Qinghai is >9% and 7%, respectively (Weijers et al., 2007; Sinninghe Damsté et al., 2012a; Liu et al., 2013b). This indicates that %thaum isomer could potentially be used to distinguish terrestrial soil iGDGT input. However, it should be noted that high %thaum isomer values in lakes are not necessarily a direct signature of terrestrial iGDGT input, since Group I.1b Thaumarchaeota can also live in lakes (e.g., Sinninghe Damsté et al., 2009). Therefore, high %thaum isomer values for lakes could indicate either a significant input from terrestrial iGDGTs or the presence of Group I.1b Thaumarchaeota, both of which could introduce bias in TEX_{86} values.

For Lake Qinghai, the GDGT-0/thaum ratio, MI index and %thaum isomer values all exhibited significant variations with time (Figs. 4c, d, e), suggesting a substantial input of iGDGTs from other sources during

certain periods (In particular, early to mid-Holocene). Consequently, TEX_{86} at these time intervals might be inapplicable for temperature reconstructions. Applying an approach similar to that used by Sinninghe Damsté et al. (2012a) in extracting reliable TEX_{86} paleotemperature from an equatorial African lake (Lake Challa), we critically excluded samples with GDGT-0/thaum > 2, MI > 0.24, or %thaum isomer > 2 for core QH-2011. About 110 data points with TEX_{86} ranging from 0.34 to 0.58 remained after filtration (Fig. 7a). Notably, these samples were mainly in the late Holocene and during 15–17 cal ka BP, when the lake was inferred to be relatively deeper and larger (Figs. 7a, b). This is in agreement with previous observations that the TEX_{86} paleothermometer appears valid primarily for large lakes (Powers et al., 2005, 2010; Tierney et al., 2008, 2010a; Woltering et al., 2011; Berke et al., 2012a, b). This is possibly because large lakes may provide a habitat suitable for aquatic Thaumarchaeota that prefer living in the relatively deeper zone in lacustrine systems, where both competition of ammonium (the substrate) from other microbes and light intensity are probably low (Tierney et al., 2010b; Schouten et al., 2013 and references therein). On the other hand, small lakes may receive much more input of terrestrial organic matter and nutrients and the hydrology of these lakes are generally unstable, causing much complexity in the origins of iGDGTs. Therefore, TEX_{86} might be only applicable for relatively larger lakes with a certain size, where iGDGTs might predominantly originate from Group I.1a aquatic Thaumarchaeota.

We tentatively apply the global lake calibration (Powers et al., 2010) to generate JLST of Lake Qinghai due to the lack of a regional calibration for TEX_{86} vs. temperature. The average reconstructed temperature for the top ~10 cm of the core (mean 15°C, n = 2) is consistent with the inferred surface water temperatures based on the U^k_{37} index (mean 15°C; Liu et al., 2008, 2011b) and the instrumental data of JLST (ca. 14.3°C; Fan et al., 1994). In fact, the warm bias in reconstructed LST based on iGDGTs has been observed for some other lakes on the QTP (Günther et al., 2014) and in New Zealand (Zink et al., 2010). Therefore, it seems reasonable to assume that the Thaumarchaeota in highland lakes grow mainly in warm months, when the lake temperature is higher, similar to the cases for other microorganisms such as the producers of long chain alkenones (Liu et al., 2008) and branched GDGTs (Sun et al., 2011; Wu et al., 2013).

Based on TEX_{86} , a dramatic drop in JLST (from 13°C to 5°C) occurred at 17.3–16.4 cal ka BP and the water temperature was coldest during 16.9–15.4 cal ka BP ($TEX_{86} < 0.4$). Such a cold-water event coincides, within dating uncertainty, with the cold event documented at ca. 15.8 ka on the adjacent Chinese Loess Plateau (in the Mangshan section; Peterse et al., 2014) and might be linked with the Heinrich 1 event widely recorded in numerous archives and proxies in the Northern Hemisphere (e.g., Heinrich, 1988; Bard et al., 2000; Wang et al., 2008). Alternatively, the cold lake water at that time was possibly due to a large proportion of melting water coming down from the surrounding mountains, as discussed above. Currently, therefore, we suggest that the cold lake temperature and highstand for Lake Qinghai at 16.9–15.4 cal ka BP may have been caused either by the low regional temperature or by inpouring of melting water resulting from increasing land temperature.

Continuous TEX_{86} -inferred JLST records for the lake were also available at the late Holocene. During this period, the temperature ($14.3 \pm 1.6^\circ\text{C}$) was substantially higher than that at 15.1–17.3 cal ka BP ($8.4 \pm 3.1^\circ\text{C}$), with several multi centennial-scale fluctuations (Fig. 7a). Due to relatively large uncertainties in our chronology, the short term fluctuations cannot be discussed in detail at present. Interestingly, we note that the TEX_{86} -inferred temperature range for Lake Qinghai during the late Holocene (9°C) is larger than that obtained for other large lakes (Lake Turkana, 2–3°C, Berke et al., 2012a; Lake Tanganyika, 4°C, Tierney et al., 2008, 2010a; Lake Malawi, 4°C, Powers et al., 2005, 2011). Such large discrepancies are possibly due to the ‘lake volume effect’ which could potentially amplify or dampen the

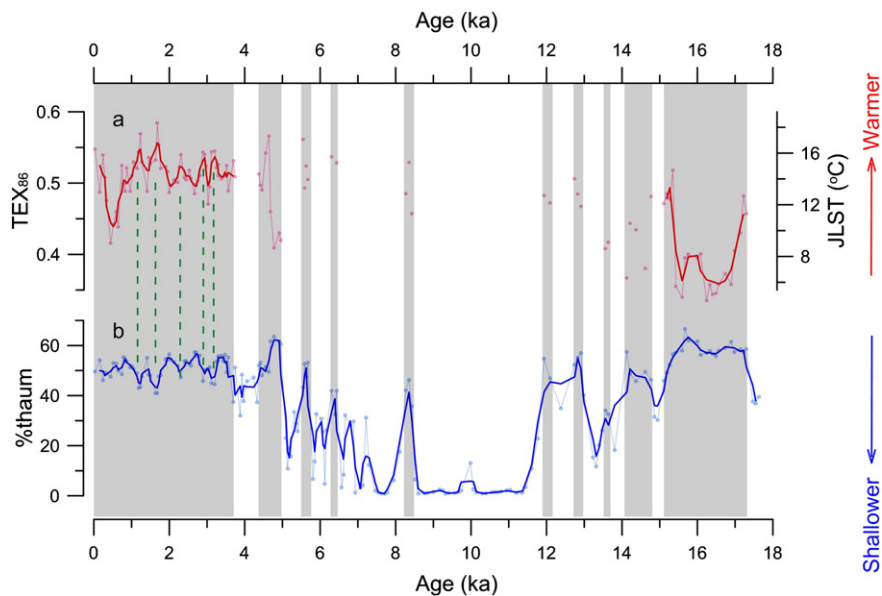


Figure 7. Temperature–hydrology association at Lake Qinghai. (a) TEX_{86} values vs. sediment age for core QH-2011 filtered via GDGT distributions (GDGT-0/thaum ratio, %thaum isomer and MI values), showing two continuous paleotemperature records at 15.1–17.3 cal ka BP and the late Holocene (the thick red lines represent the 3-point moving average). The axis on the right provides JLST estimates according to Powers et al. (2010). (b) Variation in the %thaum record with 3-point moving average. Higher %thaum values indicate higher lake levels. Periods with possibly reliable TEX_{86} values are indicated by gray shading. Generally, relatively lower lake status corresponded to warmer lake water and vice versa during the late Holocene, except for the recent 1 ka.

temperature signal recorded in lake waters (He et al., 2013a). As Lake Qinghai is not so deep as large lakes in East Africa, the oscillation in its water temperature was likely amplified. If this is the case, the quantitative estimation of late Holocene warming and cooling events from our TEX_{86} record would be challenging. However, this may not influence the temporal trend in temperature reconstructed from the TEX_{86} index, but suggests that the TEX_{86} record retrieved from Lake Qinghai might be more sensitive to regional climatic variation.

Late Holocene temperature–hydrology association for Lake Qinghai region

Because of a dearth of paleoclimate records that generate both temperature and moisture information from the same samples, independently of chronology uncertainties, our understanding in the nature of the Holocene climate pattern for the Lake Qinghai region is limited (Liu et al., 2006). The available extracted TEX_{86} record and the %thaum record for core QH-2011 during the late Holocene enable archaeal lipids to be of potential for providing further insights into the temperature–hydrology association for this region.

The two records based on archaeal lipids suggest that lake temperature and hydrological changes were generally coupled during 1–4 cal ka BP, with relatively lower lake status (presumably drier climate) corresponding to warmer lake water and vice versa (Fig. 7). This indicates a millennial-scale to centennial-scale warm–dry and cold–wet association during the 1–4 cal ka BP for the region. One might argue that when water depth reaches a threshold, %thaum may not sensitively record the water depth but may be primarily controlled by other factors such as temperature, an important factor determining TEX_{86} . However, the coupling between TEX_{86} and %thaum during 1–4 cal ka BP cannot be caused by the effect of temperature on the two indices, as they both show an increase with SST in core-top marine sediments (Kim et al., 2010), but are in an anti-phase relationship in Lake Qinghai sediments during this period.

The anti-phase relationship between lake level and temperature at Lake Qinghai possibly indicates a negative influence of temperature on effective moisture during 1–4 cal ka BP. On a larger timescale, lake level and salinity reconstructions based on multiple proxies for the lake have revealed that Lake Qinghai was shallower and more saline

at the early Holocene and became deeper and less saline towards the late Holocene (Zhang et al., 1989; Yu, 2005; Liu et al., 2013a; Wang et al., 2014), whereas local summer insolation/temperature and precipitation decreased from the early Holocene to the late Holocene (Laskar et al., 2004; An et al., 2012; Thomas et al., 2014). This phenomenon was attributed to the overweight of temperature-induced evaporation than precipitation in this region (Yu, 2005; Liu et al., 2013a; Wang et al., 2014). Additionally, the warm–dry and cold–wet association of the Holocene climate or a dry early Holocene has been widely reported from other sites on the northeastern QTP (Mischke et al., 2008; Herzsuhuh et al., 2009; He et al., 2013b; Zhao et al., 2013) and for arid/semi-arid China (Herzsuhuh, 2006; Liu et al., 2011c). Overall, for arid/semi-arid regions, the coupled temperature and hydrological variations on multiple timescales collectively support the idea that summer temperature may have played an important role in affecting regional effective moisture by controlling evapotranspiration loss (Herzsuhuh, 2006; Mischke et al., 2008; Herzsuhuh et al., 2009; Liu et al., 2013a; He et al., 2014).

For the recent ca 1 ka (particular during 0.5–0.9 cal ka BP), the climate pattern appeared different from that at 1–4 cal ka BP (Fig. 7). For instance, during the cold interval when TEX_{86} was low, the reconstructed lake level also appeared relatively low. This is possibly due to the greatly reduced rainfall during this cold interval (presumably the Little Ice Age) as a result of weakened Asian monsoons (Liu et al., 2006), despite the suppressed evapotranspiration loss resulting from low temperature. For the arid/semi-arid monsoon boundary region, therefore, hydrological response to monsoon/climatic variation could be more complex than that in monsoon-influenced humid regions, since evapotranspiration loss (induced by temperature) and precipitation are both very important factors.

Conclusions

A 5.8-m-long core from the southeast sub-basin of Lake Qinghai was investigated for the distribution of archaeal lipids, including the %thaum index, the ACE index and the TEX_{86} index, in order to extract regional hydrology and temperature signals since the late Pleistocene.

The lake-level history inferred from $\delta^{18}\text{O}$ was extended to the deglaciation, showing relatively higher lake levels at 11.9–12.9, 14.1–14.8 and 15.3–17.3 cal ka BP, except for the reported late Holocene highstand (Liu et al., 2013a; Wang et al., 2014). The reconstructed relative paleosalinity history correlated negatively with the $\delta^{18}\text{O}$ -inferred relative lake-level record, with three periods of high salinity (10.6–11.2, 13.2–13.4 and 17.4–17.6 cal ka BP) occurring when the lake was relatively shallower. Moreover, the archaeal lipid records indicate that the 15.3–17.3 cal ka BP and the late Holocene were two periods when Lake Qinghai was relatively deeper and fresher.

The TEX_{86} paleothermometer was filtered by the distributions of GDGTs to extract reliable TEX_{86} values. Periods with the extracted TEX_{86} values are all intervals when lake levels were relatively higher, suggesting that TEX_{86} might be potentially applicable predominantly for large lakes. Based on the extracted TEX_{86} , two continuous paleotemperature records were available at 15.1–17.3 cal ka BP and the late Holocene. For the 1–4 cal ka BP, we observed a strong covariation of TEX_{86} and $\delta^{18}\text{O}$ records, showing a cold/wet and warm/dry climate association on millennial to centennial scale. This supports the concept emphasizing the importance of summer temperature, in addition to monsoon precipitation, in controlling effective moisture for arid/semi-arid regions.

Overall, this study shows potential for the application of archaeal lipids in reconstructing paleoclimate and its patterns from inland lakes. However, it should be noted that the paleoenvironmental information inferred in this study was mainly based on our current knowledge of the environmental controls on the distribution of archaeal lipids. Further studies on other indices are still needed for a more comprehensive understanding of the temperature/hydrology evolution history of Lake Qinghai.

Acknowledgments

The authors would like to thank Dr. Hongxuan Lu and groups from CUGB and NIGL, CAS for help during the field work. We are also grateful to Prof. Zhisheng An, Dr. Xiangzhong Li and Dr. Zheng Wang for useful discussion. Two anonymous reviewers are thanked for their helpful comments. The research was supported by the National Natural Science Foundation of China grants #40873011 (WL), #41030211 (HD), #91028005 (CLZ), and #41002123 (HJ), National Key Funds of China #2010CB833400 (WL), and KLSLRC (KLSLRC-KF-13-DX-2). Sample analysis was completed in the State Key Laboratory of Marine Geology through the “National Thousand Talents Program” at Tongji University (CLZ).

References

An, Z., Colman, S.M., Zhou, W., Li, X., Brown, E.T., Jull, A.J.T., Cai, Y., Huang, Y., Lu, X., Chang, H., 2012. Interplay between the westerlies and Asian monsoon recorded in Lake Qinghai sediments since 32 ka. *Scientific Reports* 2. <http://dx.doi.org/10.1038/srep00619>.

Bard, E., Rostek, F., Turon, J.L., Gendreau, S., 2000. Hydrological impact of Heinrich events in the subtropical northeast Atlantic. *Science* 289, 1321–1324.

Berke, M.A., Johnson, T.C., Werne, J.P., Schouten, S., Sinninghe Damsté, J.S., 2012a. A mid-Holocene thermal maximum at the end of the African humid period. *Earth and Planetary Science Letters* 351–352, 95–104.

Berke, M.A., Johnson, T.C., Werne, J.P., Grice, K., Schouten, S., Sinninghe Damsté, J.S., 2012b. Molecular records of climate variability and vegetation response since the Late Pleistocene in the Lake Victoria basin, East Africa. *Quaternary Science Reviews* 55, 59–74.

Blaga, C.I., Reichart, G.J., Heiri, O., Sinninghe Damsté, J.S., 2009. Tetraether membrane lipid distributions in lake particulate matter and sediments: a study of 47 European lakes along a north–south transect. *Journal of Paleolimnology* 41, 523–540.

Blumenberg, M., Seifert, R., Reitner, J., Pape, T., Michaelis, W., 2004. Membrane lipid patterns typify distinct anaerobic methanotrophic consortia. *Proceedings of the National Academy of Sciences of the United States of America* 101, 11111–11116.

Brochier-Armanet, C., Boussau, B., Gribaldo, S., Forterre, P., 2008. Mesophilic crenarchaeota: proposal for a third archaeal phylum, the Thaumarchaeota. *Nature Reviews Microbiology* 6, 245–252.

Castañeda, I.S., Schouten, S., 2011. A review of molecular organic proxies for examining modern and ancient lacustrine environments. *Quaternary Science Reviews* 30, 2851–2891.

Colman, S.M., Yu, S.Y., An, Z., Shen, J., Henderson, A.C.G., 2007. Late Cenozoic climate changes in China's western interior: a review of research on Lake Qinghai and comparison with other records. *Quaternary Science Reviews* 26, 2281–2300.

De Deckker, P., Forester, R.M., 1988. The use of ostracods to reconstruct continental palaeoenvironmental records. In: De Deckker, P., Colin, J.P., Peyrouquet, J.P. (Eds.), *Ostracoda in the Earth Sciences*. Elsevier, Amsterdam, pp. 175–199.

Fan, P., Zhang, P., Ma, B., et al., 1994. Evolution of Recent Environment in Qinghai Lake and its Prediction. Science Press, Beijing, China (in Chinese).

Fu, C., An, Z., Qiang, X., Bloemendal, J., Song, Y., Chang, H., 2013. Magnetostratigraphic determination of the age of ancient Lake Qinghai, and record of the East Asian monsoon since 4.63 Ma. *Geology* 41, 875–878.

Gao, L., Nie, J., Clemens, S., Liu, W., Sun, J., Zech, R., Huang, Y., 2012. The importance of solar insolation on the temperature variations for the past 110 kyr on the Chinese Loess Plateau. *Palaeogeography, Palaeoclimatology, Palaeoecology* 317–318, 128–133.

Günther, F., Thiele, A., Gleixner, G., Xu, B., Yao, T., Schouten, S., 2014. Distribution of bacterial and archaeal ether lipids in soils and surface sediments of Tibetan lakes: implications for GDGT-based proxies in saline high mountain lakes. *Organic Geochemistry* 67, 19–30.

He, Y., Liu, W., Zhao, C., Wang, Z., Wang, H., Liu, Y., Qin, X., Hu, Q., An, Z., Liu, Z., 2013a. Solar influenced late Holocene temperature changes on the northern Tibetan Plateau. *Chinese Science Bulletin* 58, 1053–1059.

He, Y., Zhao, C., Wang, Z., Wang, H., Song, M., Liu, W., Liu, Z., 2013b. Late Holocene coupled moisture and temperature changes on the northern Tibetan Plateau. *Quaternary Science Reviews* 80, 47–57.

He, Y., Zheng, Y., Pan, A., Zhao, C., Sun, Y., Song, M., Zheng, Z., Liu, Z., 2014. Biomarker-based reconstructions of Holocene lake-level changes at Lake Gahai on the northeastern Tibetan Plateau. *The Holocene* <http://dx.doi.org/10.1177/0959683613519689>.

Heinrich, H., 1988. Origin and consequences of cyclic ice rafting in the northeast Atlantic Ocean during the past 130,000 years. *Quaternary Research* 29, 142–152.

Henderson, A.C.G., Holmes, J.A., 2009. Palaeolimnological evidence for environmental change over the past millennium from Lake Qinghai sediments: a review and future research perspective. *Quaternary International* 194, 134–147.

Henderson, A.C.G., Holmes, J.A., Leng, M.J., 2010. Late Holocene isotope hydrology of Lake Qinghai, NE Tibetan Plateau: effective moisture variability and atmospheric circulation changes. *Quaternary Science Reviews* 29, 2215–2223.

Herzschuh, U., 2006. Palaeo-moisture evolution at the margins of the Asian monsoon during the last 50 ka. *Quaternary Science Reviews* 25, 163–178.

Herzschuh, U., Kramer, A., Mischke, S., Zhang, C., 2009. Quantitative climate and vegetation trends since the late glacial on the northeastern Tibetan Plateau deduced from Koucha Lake pollen spectra. *Quaternary Research* 71, 162–171.

Hopmans, E.C., Schouten, S., Pancost, R.D., van der Meer, M.T.J., Sinninghe Damsté, J.S., 2000. Analysis of intact tetraether lipids in archaeal cell material and sediments by high performance liquid chromatography/atmospheric pressure chemical ionization mass spectrometry. *Rapid Communications in Mass Spectrometry* 14, 585–589.

Huguet, C., Hopmans, E.C., Febo-Ayala, W., Thompson, D.H., Sinninghe Damsté, J.S., Schouten, S., 2006. An improved method to determine the absolute abundance of glycerol dibiphytanyl glycerol tetraether lipids. *Organic Geochemistry* 37, 1036–1041.

Huguet, A., Fosse, C., Metzger, P., Fritsch, E., Derenne, S., 2010. Occurrence and distribution of non-extractable glycerol dialkyl glycerol tetraethers in temperate and tropical podzol profiles. *Organic Geochemistry* 41, 833–844.

Ji, J., Shen, J., Balsam, W., Chen, J., Liu, L., Liu, X., 2005. Asian monsoon oscillations in the northeastern Qinghai–Tibet Plateau since the late glacial as interpreted from visible reflectance of Qinghai Lake sediments. *Earth and Planetary Science Letters* 233, 61–70.

Jia, G., Rao, Z., Zhang, J., Li, Z., Chen, F., 2013. Tetraether biomarker records from a loesspaleosol sequence in the western Chinese Loess Plateau. *Frontiers in Microbiology* 4.

Kim, J.-H., van der Meer, J., Schouten, S., Helmke, P., Willmott, V., Sangiorgi, F., Koç, N., Hopmans, E.C., Sinninghe Damsté, J.S., 2010. New indices and calibrations derived from the distribution of crenarchaeal isoprenoid tetraether lipids: implications for past sea surface temperature reconstructions. *Geochimica et Cosmochimica Acta* 74, 4639–4654.

Laskar, J., Robutel, P., Joutel, F., Gastineau, M., Correia, A.C.M., Levrard, B., 2004. A long-term numerical solution for the insolation quantities of the Earth. *Astronomy and Astrophysics* 428, 261–285.

Li, X., Liu, W., 2014. Water salinity and productivity recorded by ostracod assemblages and their carbon isotopes since the early Holocene at Lake Qinghai on the northeastern Qinghai–Tibet Plateau, China. *Palaeogeography, Palaeoclimatology, Palaeoecology* 407, 25–33.

Lister, G., Kelts, K., Chen, K.Z., Yu, J.Q., Niessen, F., 1991. Lake Qinghai, China: closed-basin lake levels and the oxygen isotope record for ostracoda since the latest Pleistocene. *Palaeogeography, Palaeoclimatology, Palaeoecology* 84, 141–162.

Liu, Z., Henderson, A.C.G., Huang, Y., 2006. Alkenone-based reconstruction of late-Holocene surface temperature and salinity changes in Lake Qinghai, China. *Geophysical Research Letters* 33, L09707. <http://dx.doi.org/10.1029/2006GL026151>.

Liu, W., Liu, Z., Fu, M., An, Z., 2008. Distribution of the C_{37} tetra-unsaturated alkenone in Lake Qinghai, China: a potential lake salinity indicator. *Geochimica et Cosmochimica Acta* 72, 988–997.

Liu, Z., Pagani, M., Zinniker, D., DeConto, R., Huber, M., Brinkhuis, H., Shah, S.R., Leckie, M., Pearson, A., 2009. Global cooling during the Eocene–Oligocene climate transition. *Science* 323, 1187–1190.

Liu, X.J., Lai, Z.P., Yu, L.P., Liu, K., Zhang, J.R., 2011a. Lake level variations of Qinghai Lake in northeastern Qinghai–Tibet Plateau since 3.7 ka based on OSL dating. *Quaternary International* 236, 57–64.

Liu, W., Liu, Z., Wang, H., He, Y., Wang, Z., Xu, L., 2011b. Salinity control on long-chain alkenone distributions in lake surface waters and sediments of the northern Qinghai–Tibetan Plateau, China. *Geochimica et Cosmochimica Acta* 75, 1693–1703.

- Liu, W., Liu, Z., An, Z., Wang, X., Chang, H., 2011c. Wet climate during the 'Little Ice Age' in the arid Tarim Basin, northwestern China. *The Holocene* 21, 409–416.
- Liu, W., Li, X., An, Z., Xu, L., 2013a. Total organic carbon isotopes: a novel proxy of lake level from Lake Qinghai in the Qinghai–Tibet Plateau, China. *Chemical Geology* 347, 153–160.
- Liu, W., Wang, H., Zhang, C.L., Liu, Z., He, Y., 2013b. Distribution of glycerol dialkyl glycerol tetraether lipids along an altitudinal transect on Mt. Xiangpi, NE Qinghai–Tibetan Plateau, China. *Organic Geochemistry* 57, 76–83.
- Lu, H., Zhao, C., Mason, J., Yi, S., Zhao, H., Zhou, Y., Ji, J., Swinehart, J., Wang, C.M., 2011. Holocene climate changes revealed by Aeolian deposits from the Qinghai Lake area (northeastern Qinghai–Tibetan Plateau) and possible forcing mechanisms. *The Holocene* 21, 297–304.
- LZBCAS (Lanzhou Branch Chinese Academy of Sciences), 1994. Evolution of recent environment in Qinghai Lake and its prediction. West Center of Resource and Environment, Chinese Academy of Sciences. Science Press, Beijing, China (in Chinese).
- Ménot, G., Bard, E., 2012. A precise search for drastic temperature shifts of the past 40,000 years in southeastern Europe. *Paleoceanography* 27 PA2210.
- Mischke, S., Kramer, M., Zhang, C., Shang, H., Herzsich, U., Erzinger, J., 2008. Reduced early Holocene moisture availability in the Bayan Har Mountains, northeastern Tibetan Plateau, inferred from a multi-proxy lake record. *Palaeogeography, Palaeoclimatology, Palaeoecology* 267, 59–76.
- Pancost, R., Hopmans, E.C., Sinninghe Damsté, J.S., Medinauth Scientific Party, 2001. Archaeal lipids in Mediterranean cold seeps: molecular proxies for anaerobic methane oxidation. *Geochimica et Cosmochimica Acta* 65, 1611–1627.
- Pearson, A., Ingalls, A.E., 2013. Assessing the use of archaeal lipids as marine environmental proxies. *Annual Review of Earth and Planetary Sciences* 41, 359–384.
- Pearson, E.J., Juggins, S., Talbot, H.M., Weckström, J., Rosén, P., Ryves, D.B., Roberts, S.J., Schmidt, R., 2011. A lacustrine GDGT-temperature calibration from the Scandinavian Arctic to Antarctica: renewed potential for the application of GDGT-paleothermometry in lakes. *Geochimica et Cosmochimica Acta* 75, 6225–6238.
- Peterse, F., Prins, M.A., Beets, C.J., Troelstra, S.R., Zheng, H., Gu, Z., Schouten, S., Sinninghe Damsté, J.S., 2011. Decoupled warming and monsoon precipitation in East Asia over the last deglaciation. *Earth and Planetary Science Letters* 301, 256–264.
- Peterse, F., Martínez-García, A., Zhou, B., Beets, C.J., Prins, M.A., Zheng, H., Eglinton, T.I., 2014. Molecular records of continental air temperature and monsoon precipitation variability in East Asia spanning the past 130,000 years. *Quaternary Science Reviews* 83, 1–7.
- Pitcher, A., Rychlik, N., Hopmans, E.C., Spieck, E., Rijpstra, W.I.C., Ossebaar, J., Schouten, S., Wagner, M., Sinninghe Damsté, J.S., 2010. Crenarchaeol dominates the membrane lipids of *Candidatus Nitrososphaera gargensis*, a thermophilic Group I.1b Archaeon. *The ISME Journal* 4, 542–552.
- Pitcher, A., Hopmans, E.C., Mosier, A.C., Francis, C.A., Reese, S.K., Schouten, S., Sinninghe Damsté, J.S., 2011. Core and intact polar glycerol dibiphytanyl glycerol tetraether lipids of ammonia-oxidizing archaea enriched from marine and estuarine sediments. *Applied and Environmental Microbiology* 77, 3468–3477.
- Powers, L.A., Werne, J.P., Johnson, T.C., Hopmans, E.C., Sinninghe Damsté, J.S., Schouten, S., 2004. Crenarchaeotal membrane lipids in lake sediments: a new paleotemperature proxy for continental paleoclimate reconstruction? *Geology* 32, 613–616.
- Powers, L.A., Johnson, T.C., Werne, J.P., Castañeda, I.S., Hopmans, E.C., Sinninghe Damsté, J.S., Schouten, S., 2005. Large temperature variability in the southern African tropics since the Last Glacial Maximum. *Geophysical Research Letters* 32 L08706.
- Powers, L., Werne, J.P., Vanderwoude, A.J., Sinninghe Damsté, J.S., Hopmans, E.C., Schouten, S., 2010. Applicability and calibration of the TEX₈₆ paleothermometer in lakes. *Organic Geochemistry* 41, 404–413.
- Powers, L.A., Werne, J.P., Castañeda, I.S., Johnson, T.C., Hopmans, E.C., Sinninghe Damsté, J.S., Schouten, S., 2011. Organic geochemical records of environmental variability in Lake Malawi (East Africa) during the last 700 years, Part I: the TEX₈₆ temperature record. *Palaeogeography Palaeoclimatology Palaeoecology* 303, 133–139.
- Reimer, P.J., Bard, E., Bayliss, A., Beck, J.W., Blackwell, P.G., Bronk Ramsey, C., Buck, C.E., Cheng, H., Edwards, R.L., Friedrich, M., Grootes, P.M., Guilderson, T.P., Haffidson, H., Hajdas, I., Hatté, C., Heaton, T.J., Hoffman, D.L., Hogg, A.G., Hughen, K.A., Kaiser, K.F., Kromer, B., Manning, S.W., Niu, M., Reimer, R.W., Richards, D.A., Scott, E.M., Southon, J.R., Staff, R.A., Turney, C.S.M., van der Plicht, J., 2013. IntCal13 and Marine13 radiocarbon age calibration curves 0–50,000 years cal BP. *Radiocarbon* 55, 1869–1887.
- Schouten, S., Hopmans, E.C., Schefuss, E., Sinninghe Damsté, J.S., 2002. Distributional variations in marine crenarchaeotal membrane lipids: a new tool for reconstructing ancient sea water temperatures? *Earth and Planetary Science Letters* 204, 265–274.
- Schouten, S., Hopmans, E.C., Kuypers, M.M.M., van Breugel, Y., Forster, A., Sinninghe Damsté, J.S., 2003. Extremely high sea water temperatures at low latitudes during the middle Cretaceous as revealed by archaeal membrane lipids. *Geology* 31, 1069–1072.
- Schouten, S., Huguet, C., Hopmans, E.C., Sinninghe Damsté, J.S., 2007. Improved analytical methodology of the TEX₈₆ paleothermometry by high performance liquid chromatography/atmospheric pressure chemical ionization–mass spectrometry. *Analytical Chemistry* 79, 2940–2944.
- Schouten, S., Rijpstra, W.I.C., Schubert, C.J., Durisch-Kaiser, E., Sinninghe Damsté, J.S., 2012. Distribution of glycerol dialkyl glycerol tetraether lipids in the water column of Lake Tanganyika. *Organic Geochemistry* 53, 34–37.
- Schouten, S., Hopmans, E.C., Sinninghe Damsté, J.S., 2013. The organic geochemistry of glycerol dialkyl glycerol tetraether lipids: a review. *Organic Geochemistry* 54, 19–61.
- Shen, J., Liu, X., Wang, S., Matsumoto, R., 2005. Palaeoclimatic changes in the Qinghai Lake area during the last 18,000 years. *Quaternary International* 136, 131–140.
- Shi, Y., Lu, M., Li, W., 1958. Physical geography with emphasis on geomorphology around Lake Qinghai. *Acta Geographica Sinica* 24, 33–48 (in Chinese).
- Sinninghe Damsté, J.S., Schouten, S., Hopmans, E.C., van Duin, A.C.T., Geenevaans, J.A.J., 2002. Crenarchaeol: the characteristic core glycerol dibiphytanyl glycerol tetraether membrane lipid of cosmopolitan pelagic crenarchaeota. *Journal of Lipid Research* 43, 1641–1651.
- Sinninghe Damsté, J.S., Ossebaar, J., Abbas, B., Schouten, S., Verschuren, D., 2009. Fluxes and distribution of tetraether lipids in an equatorial African lake: constraints on the application of the TEX₈₆ paleothermometer and branched tetraether lipids in lacustrine settings. *Geochimica et Cosmochimica Acta* 73, 4232–4249.
- Sinninghe Damsté, J.S., Ossebaar, J., Schouten, S., Verschuren, D., 2012a. Distribution of tetraether lipids in the 25-ka sedimentary record of Lake Challa: extracting reliable TEX₈₆ and MBT/CBT paleotemperatures from an equatorial African lake. *Quaternary Science Reviews* 50, 43–54.
- Sinninghe Damsté, J.S., Rijpstra, W.I.C., Hopmans, E.C., Man-Young, Jung, Jong-Geol, Kim, Rhee, S.-K., Stieglmeier, M., Schleper, C., 2012b. Intact polar and core glycerol dibiphytanyl glycerol tetraether lipids of group 1.1a and 1.1b ammonia-oxidizing archaea in soil. *Applied and Environmental Microbiology* 78, 6866–6874.
- Spang, A., Hatzenpichler, R., Brochier-Armanet, C., Rattai, T., Tischler, P., Spieck, E., Streit, W., Stahl, D.A., Wagner, M., Schleper, C., 2010. Distinct gene set in two different lineages of ammonia-oxidizing archaea supports the phylum Thaumarchaeota. *Trends in Microbiology* 18, 331–340.
- Sun, Q., Chu, G., Liu, M., Xie, M., Li, S., Ling, Y., Wang, X., Shi, L., Jia, G., Lü, H., 2011. Distributions and temperature dependence of branched glycerol dialkyl glycerol tetraethers in recent lacustrine sediments from China and Nepal. *Journal of Geophysical Research* 116 G01008.
- Thomas, E.K., Huang, Y., Morrill, C., Zhao, J., Wegener, P., Clemens, S., Colman, S., Gao, L., 2014. Abundant C₄ plants on the Tibetan Plateau during the late glacial and early Holocene. *Quaternary Science Reviews* 87, 24–33.
- Thompson, L.G., Yao, T.D., Davis, M.E., Henderson, K.A., Mosley-Thompson, E., Lin, P.-N., Beer, J., Synal, H.-A., Cole-Dai, J., Bolzan, J.F., 1997. Tropical climate instability: the last glacial cycle from a Qinghai–Tibetan ice core. *Science* 276, 1821–1825.
- Tierney, J.E., Russell, J.M., Huang, Y., Sinninghe Damsté, J.S., Hopmans, E.C., Cohen, A.S., 2008. Northern hemisphere controls on tropical southeast African climate during the past 60,000 years. *Science* 322, 252–255.
- Tierney, J.E., Mayes, M.T., Meyer, N., Johnson, C., Swarzenski, P.W., Cohen, A.S., Russell, J.M., 2010a. Late-twentieth-century warming in Lake Tanganyika unprecedented since AD 500. *Nature Geoscience* 3, 422–425.
- Tierney, J.E., Russell, J.M., Eggermont, H., Hopmans, E.C., Verschuren, D., Sinninghe Damsté, J.S., 2010b. Environmental controls on branched tetraether lipid distributions in tropical East African lake sediments. *Geochimica et Cosmochimica Acta* 74, 4902–4918.
- Turich, C., Freeman, K.H., 2011. Archaeal lipids record paleosalinity in hypersaline systems. *Organic Geochemistry* 42, 1147–1157.
- Wakeham, S.G., Lewis, C.A., Hopmans, E.C., Schouten, S., Sinninghe Damsté, J.S., 2003. Archaea mediate anaerobic oxidation of methane in deep euxinic waters of the Black Sea. *Geochimica et Cosmochimica Acta* 67, 1359–1374.
- Wang, Y., Cheng, H., Edwards, R.L., Kong, X.G., Shao, X., Chen, S., Wu, J., Jiang, X., Wang, X., An, Z., 2008. Millennial- and orbital-scale changes in the East Asian monsoon over the past 224,000 years. *Nature* 451, 1090–1093.
- Wang, Y., Shen, J., Xu, X., Liu, X., Sirocko, F., Zhang, E., Ji, J., 2011. Environmental changes during the past 13500 cal. a BP deduced from lacustrine sediment records of Lake Qinghai, China. *Chinese Journal of Geochemistry* 30, 479–489.
- Wang, H., Liu, W., Zhang, C.L., Wang, Z., Wang, J., Liu, Z., Dong, H., 2012. Distribution of glycerol dialkyl glycerol tetraethers in surface sediments of Lake Qinghai and surrounding soil. *Organic Geochemistry* 47, 78–87.
- Wang, H., Liu, W., Zhang, C.L., Jiang, H., Dong, H., Lu, H., Wang, J., 2013. Assessing the ratio of archaeal to caldarchaeol as a salinity proxy in highland lakes on the northeastern Qinghai–Tibetan Plateau. *Organic Geochemistry* 54, 69–77.
- Wang, H., Dong, H., Zhang, C.L., Jiang, H., Zhao, M., Liu, Z., Lai, Z., Liu, W., 2014. Water depth affecting thaumarchaeol production in Lake Qinghai, northeastern Qinghai–Tibetan plateau: implications for paleo lake levels and paleoclimate. *Chemical Geology* 368, 76–84.
- Weijers, J.W.H., Schouten, S., Spaargaren, O.C., Sinninghe Damsté, J.S., 2006. Occurrence and distribution of tetraether membrane lipids in soils: implications for the use of the BIT index and the TEX₈₆ SST proxy. *Organic Geochemistry* 37, 1680–1693.
- Weijers, J.W.H., Schouten, S., van den Donker, J.C., Hopmans, E.C., Sinninghe Damsté, J.S., 2007. Environmental controls on bacterial tetraether membrane lipid distribution in soils. *Geochimica et Cosmochimica Acta* 71, 703–713.
- Williams, W.D., 1991. Chinese and Mongolian saline lakes: a limnological overview. *Hydrobiologia* 210, 39–66.
- Woltering, M., Johnson, T.C., Werne, J.P., Schouten, S., Sinninghe Damsté, J.S., 2011. Late Pleistocene temperature history of Southeast Africa: a TEX₈₆ temperature record from Lake Malawi. *Palaeogeography, Palaeoclimatology, Palaeoecology* 303, 93–102.
- Wu, X., Dong, H.L., Zhang, C.L., Liu, X., Hou, W., Zhang, J., Jiang, H., 2013. Evaluation of glycerol dialkyl glycerol tetraether proxies for reconstruction of the paleo-environment on the Qinghai–Tibetan Plateau. *Organic Geochemistry* 61, 45–56.
- Xie, S., Pancost, R.D., Chen, L., Evershed, R.P., Yang, H., Zhang, K., 2012. Microbial lipid records of highly alkaline deposits and enhanced aridity associated with significant uplift of the Tibetan Plateau in the Late Miocene. *Geology* 40, 291–294.
- Xu, H., Hou, Z., An, Z., Liu, X., Dong, J., 2010. Major ion chemistry of waters in Lake Qinghai catchments, NE Qinghai–Tibet plateau, China. *Quaternary International* 212, 35–43.
- Yang, H., Ding, W., Wang, J., Jin, C., He, G., Qin, Y., Xie, S., 2012. Soil pH impact on microbial tetraether lipids and terrestrial input index (BIT) in China. *Science China Earth Sciences* 55, 236–245.
- Yang, H., Pancost, R.D., Tang, C., Ding, W., Dang, X., Xie, S., 2014. Distributions of isoprenoid and branched glycerol dialkanol diethers in Chinese surface soils and a loess-paleosol sequence: implications for the degradation of tetraether lipids. *Organic Geochemistry* 66, 70–79.

- Yu, J.Q., 2005. Lake Qinghai, China: A multi-proxy investigation on sediment cores for the reconstructions of paleoclimate and paleoenvironment since the Marine Isotope Stage 3. Dissertation, Faculty of Materials and Geoscience, Technical University of Darmstadt.
- Zachos, J.C., Schouten, S., Bohaty, S., Quattlebaum, T., Sluijs, A., Brinkhuis, H., Gibbs, S., Bralower, T., 2006. Extreme warming of mid-latitude coastal ocean during the Paleocene–Eocene thermal maximum: inferences from TEX₈₆ and isotope data. *Geology* 34, 737–740.
- Zhang, P., Zhang, B., Yang, W., 1989. On the model of post-glacial palaeoclimatic fluctuation in Qinghai Lake region. *Quaternary Sciences* 9, 66–77 (in Chinese).
- Zhang, P.X., Zhang, B.Z., Qian, G.M., Li, H.J., Xu, L.M., 1994. The study of Paleoclimatic parameter of Qinghai Lake since Holocene. *Quaternary Sciences* 3, 225–236 (in Chinese with English abstract).
- Zhang, C.L., Pancost, R.D., Qian, Y., Sassen, R., Macko, S.A., 2003. Archaeal lipid biomarkers and isotopic evidence of anaerobic methane oxidation associated with gas hydrates in the Gulf of Mexico. *Organic Geochemistry* 34, 827–834.
- Zhang, Y., Zhang, C.L., Liu, X., Li, L., Hinrichs, K.U., Noakes, J.E., 2011. Methane Index: a tetraether archaeal lipid biomarker indicator for detecting the instability of marine gas hydrates. *Earth and Planetary Science Letters* 307, 525–534.
- Zhang, C.L., Wang, J., Wei, Y., Zhu, C., Huang, L., Dong, H., 2012. Production of branched tetraether lipids in the lower Pearl River and estuary: effects of extraction methods and impact on bGDGT proxies. *Frontiers in Microbiology* 2. <http://dx.doi.org/10.3389/fmicb.2011.00274>.
- Zhao, C., Liu, Z., Rohling, E.J., Yu, Z., Liu, W., He, Y., Zhao, Y., Chen, F., 2013. Holocene temperature fluctuations in the northern Tibetan Plateau. *Quaternary Research* 80, 55–65.
- Zink, K.J., Vandergous, M.J., Mangelsdorf, K., Dieffenbacher, A.C., Schwark, L., 2010. Application of bacterial glycerol dialkyl glycerol tetraethers (GDGTs) to develop modern and past temperature estimates from New Zealand lakes. *Organic Geochemistry* 41, 1060–1066.